(1)

MULTIPLE ELECTRODE ANALYSIS OF THE SYNCHRONOUS SPATIOTEMPORAL PATTERNS OF PURKINJE CELL COMPLEX SPIKE ACTIVITY IN MAMMALIAN CEREBELLUM

TOYAMA MEDICAL AND PHARMACEUTICAL UNIVERSITY

MASAJI FUKUDA

MULTIPLE ELECTRODE ANALYSIS OF THE SYNCHRONOUS SPATIOTEMPORAL PATTERNS OF PURKINJE CELL COMPLEX SPIKE ACTIVITY IN MAMMALIAN CEREBELLUM

M. FUKUDA†, T. YAMAMOTO* and R. LLINAS**

Department of Physiology and Biophysics, New York University Medical Center, 550 First Avenue, New York, NY 10016, U.S.A.

Running title: Spatiotemporal relationships in multiple recording

Present address:
†Department of Physiology, Faculty of Medicine, Toyama Medical and Pharmaceutical University, Sugitani, Toyama 930-01, Japan.
*Department of Otorhinolaryngology, Faculty of Medicine, Kyushu University, Fukuoka 812, Japan.

**To whom correspondence should be addressed.

Abstract

Complex spike activity in Purkinje cells in rat cerebellar cortex was studied utilizing multiple electrode recording techniques. Two approaches were used to analyze spatiotemporal relationships within the complex data arrays recorded during these experiments: a) grouping cells with similar spatiotemporal firing patterns via the projection method and b) so-called principal component analysis. The grouping technique enabled the visualization of relationships within an entire neuron set, through the projection of cross-correlation vectors from hyperdimensional to lower dimensional space. Each cluster of cross-correlation vectors corresponded well to the rostrocaudal organization of climbing fiber activity in cerebellar cortex. Application of principal component multivariate analysis revealed major components of complex spatiotemporal variance in climbing fiber activity of multiple Purkinje cells. A maximum variance of 30% may be ascribed to the first and second components, which corresponded, respectively, to synchronicity and spatial grouping in the spatiotemporal organization. These analyses permitted a global and quantitative description of the simultaneous activity of groups of individual neurons.

Previous multi-electrode studies of cerebellar Purkinje cell activity analyzed temporal interactions between different folia oriented in a rostrocaudal band and between folia in different parts of the rat cerebellar cortex[18]. As the number of cells recorded increases from 32 in our first studies[16] to 96[18], more sophisticated methods of data analysis have been required. Recently, multichannel neuronal activity has been recorded using optical measurements[6] as well as multiple microelectrode[1,9]. However, methods for the analysis of such complex multiple neuronal activity is still lacking[5,9]. This paper details two techniques: a) projection method and b) principal component analysis. The latter is often applied to analyze the magnitude of responses to various stimuli[2,3,8]. Preliminary reports have been presented[4,17].

EXPERIMENTAL PROCEDURES

Database

The experimental procedures and the database for this paper have been described in detail[18]. However, in the present study, all data comprising 64 and 96 bit structures were reconstructed using a 10-msec sampling rather than the 1-msec sampling used in the previous analysis[18].

Cross-correlation

To ascertain the relationship between the activities of two given neurons with x(t) and y(t) spike trains, a cross-correlation function was calculated as described in a previous paper[16]:

$$\zeta_{xy}(\tau) = \frac{\phi_{xy}(\tau) - XY\left(\frac{\Delta\tau}{T}\right)}{\sqrt{\left(\sum_{i=1}^{n} X_i^2 - X^2\frac{\Delta\tau}{T}\right)\left(\sum_{i=1}^{n} Y_i^2 - Y^2\frac{\Delta\tau}{T}\right)}} \qquad (1)$$

where X_i and Y_i represent number of spikes in x(t) and y(t) during τ_i, respectively. $X(\Delta\tau/T)$ and $Y(\Delta\tau/T)$ are the mean number of spikes in x(t) and y(t) during T, respectively; n is the total number of τ_i during T; $\phi_{XY}(\tau)$ is the number of spikes in a given lag time, τ, of the cross-correlation in the spike trains of x(t) and y(t).

Cross-correlation coefficients were calculated over a maximum time span of -250 to 250 msec and for a possible combination of any two neurons; ${}_{48}C_2$=1128 pairs for 48 neurons in one cerebellar hemisphere and ${}_{96}C_2$=4560 pairs for 96 neurons in both hemispheres. The maximum coefficient over this time span was chosen as the coefficient from one complex spike train (master neuron) to another (sub-neuron); usually the coefficient value was maximum at time lag τ=0. A correlation matrix, C, was thus calculated automatically from this procedure.

Projection method

The level of activity of a given neuron with respect to another neuron may be represented by a cross-correlation as a function of time lag. When the activity of many neurons is recorded simultaneously, it is difficult to determine the relationship among the individual cells. One way to represent such data is to use the projection method (Fig. 1A). If each element of the cross-correlation matrix is considered to be an activity vector component, as:

$$C_i = (C_{i1}, C_{i2}, \ldots\ldots, C_{iN}) \qquad (2)$$

where N is the number of recorded neurons (Fig. 1Ab), each cross-correlation vector may then be plotted as a point (a vector) in the N-dimensional space providing a succinct quantitative description of the overall activity (Fig. 1Ac). After calculating all the cross-correlation pairs possible for the recorded neurons, a total of N-points of cross-correlation vectors may be plotted on the N-dimensional space (Fig. 1Ac). The relative distance between the vectors will then describe the similarity of firing among different neurons.

Our objective was to determine the distribution of these points in the N-dimensional space. One way to simplify and visualize the distribution is to project the vectors from N-dimensional space to two- or three-dimensional space. If we define the correlation vector to be:

$$\mathbf{p}=C\mathbf{k} \qquad (3)$$

where $\mathbf{k}$ is the unit vector, and if we determine their directions of projection, the variance of vector $\mathbf{p}$ may be obtained:

$$\mathrm{Var}(\mathbf{p}) = \mathbf{k}'C^2\mathbf{k}$$

where the apostrophe indicates the transformation of $\mathbf{k}$. The unit vector $\mathbf{k}$ with the maximum variance is calculated by a characteristic equation:

$$C^2\mathbf{k} = \lambda\mathbf{k}.$$

Solving this equation gives the eigenvalue and eigenvector for the matrix C^2. The eigenvector is the same as that for matrix C, while the eigenvalue, λ, is the square of that for matrix C. It is evident, then, that the projections of N-points on a lower dimensional space are given by vector $\mathbf{p}$ of a lower dimensional space, where the eigenvalue is taken to be the largest value. When a set of points on

an N-dimensional space is projected on a two-dimensional plane, only the first and second eigenvectors are used (Figs. 1Ac and 3).

Principal component analysis

Firing patterns recorded in multi-electrode experiments demonstrate a high level of variability in time and space. Thus a procedure able to extract patterns from a large volume of data would be most welcome. It is well-known that principal component analysis is one of the most useful methods to extract invariance in a statistical field[7,14]. There is a difference, however, in applying such analysis to recordings of neuronal activity and the statistical data used in standard textbooks. One important difference is that in the multivariate analyses of statistics, the raw data does not include null points while neuronal data sets contain many such points when neurons are silent. In the following we applied a procedure similar to principal component analysis to neuronal data.

Sampling data from multiple electrode recordings may be regarded as measurements taken on P different trials (recording time) for N different variables (number of recorded neurons), where trials are defined as a function of time. An entire data set may thus be placed in a P x N data matrix composed of 1 or 0 elements as:

$$\mathbf{X} = (x_{ij}) \quad \text{where } x_{ij} = 1 \text{ or } 0, \quad i = 1...P, \; j = 1....N \qquad (4)$$

although the matrix involves null data sets when all the neurons are silent at a given moment (Fig. 1B). The mean firing frequency and standard deviation of spontaneous activity is usually different among neurons. To simplify the analysis a new variable, Z_{ij}, is introduced, allowing the original data to be standardized such that

the mean firing frequency for all the cells is identical and has a standard deviation of 1. Thus, the new variable, Z_{ij}, is:

$$Z_{ij} = \frac{(x_{ij} - \overline{x_j})}{\sqrt{\frac{1}{P}\sum_{m=1}^{P}(x_{mj} - \overline{x_j})^2}}, \quad \text{where} \quad \overline{x_j} = \frac{1}{P}\sum_{m=1}^{P} x_{mj} \qquad (5)$$

Using this new variable we can calculate a correlation matrix, C, in which each element is:

$$C_{ij} = \frac{\sum_{m=1}^{P}(x_{mi} - \overline{x_i})(x_{mj} - \overline{x_j})}{\sqrt{\sum_{m=1}^{P}(x_{mi} - \overline{x_i})^2 \sum_{m=1}^{P}(x_{mj} - \overline{x_j})^2}} \qquad i, j = 1, \ldots\ldots, N \qquad (6)$$

This definition is similar to the formula for the cross-correlation at time lag = 0 defined in eq. (1).

Principal component analysis seeks to explain the variance-covariance structure of data sets by using linear combinations of original variables, that is, to account for the variability by identifying a small number of principal components. The theoretical basis and analytical details of this type of analysis are described in many standard textbooks[7,14].

Briefly, consider the linear combinations:

$$y_i = k_{i1}Z_1 + k_{i2}Z_2 + \ldots\ldots + k_{iN}Z_N \qquad (7)$$

where $Z_i = (Z_{i1}, Z_{i2}, \ldots\ldots, Z_{iN})$ is the column vector of a standardized data matrix and **k** is a directional unit vector.

The variance of **y** is given to be:

$$\text{Var}(y) = \mathbf{k}' \, C \, \mathbf{k}.$$

The principal components are those uncorrelated linear combinations y_i whose variance is as large as possible. The first component is the linear combination with maximum variance. The solution of the direction vector **k** is the eigenvector of correlation

matrix C. The eigenvalue is equal to the variance of the correlation matrix. For maximum variance we must take the largest eigenvalue, which corresponds to the first principal component. The second largest eigenvalue corresponds to the second principal component.

The eigenvalue and its corresponding eigenvector cannot usually be estimated as analytical means. In the case of special structures with uniform correlation matrices, the largest eigenvalue, λ_1, can be estimated to be:

$$\lambda_1 = 1 + (N-1)\varrho \qquad (8)$$

where ϱ is an element of the uniform correlation matrix. Noted that if $N >> 1$, the largest eigenvalue is proportional to $N\varrho$.

RESULTS

Spatial distribution of the cross-correlation coefficient value

Several large data sets were obtained during multiple-electrode experiments in the cerebellar cortex. The number of recording electrodes, drugs applied and right or left recording locations were variable. Table 1 summarizes the mean values of the spontaneous firing frequency, cross-correlation coefficient and its standard deviation (SD) among neuronal pairs in 42 typical measurements in three experiments using 64 electrodes and 40 typical measurements from three experiments using 96 electrodes. Note that since the sampling interval was 10-msec the cross-correlation coefficients were larger than those described previously, where a 1-msec sampling interval was used[18]. The firing characteristics of Purkinje cells recorded in the 64- and 96-electrode were similar to each other, as were those of cells recorded from either hemisphere. A data set obtained during a typical

electrode experiment was analyzed. The other data, included in Table 1, exhibited similar characteristics.

Figure 2 is a typical example of the spatial distribution of the cross-correlation of spontaneous activity (spont) and activity after application of harmaline (harm) and picrotoxin (PTX) in the right and left hemispheres (a right hemisphere neuron was chosen as the master neuron, M, in Fig. 2). The mean cross-correlation coefficients and SD were 0.071 ± 0.060, 0.168 ± 0.146, and 0.230 ± 0.109 in the right site; and 0.064 ± 0.065, 0.197 ± 0.139 and 0.254 ± 0.117 in the left site for spontaneous, harmaline and picrotoxin (PTX) cases, respectively. The larger dots corresponding to large correlation coefficients, reveal a rostrocaudal organization of spontaneous activity with respect to the master neuron on the surface of Crus IIA. This organization is enhanced after application of harmaline. The bandwidth of the region of the highest correlation was about 500 μm. The cross-correlation coefficients were largest after picrotoxin application and its distribution became relatively uniform [mean SD/mean cross-correlation = 0.47 (right); 0.46 (left) in PTX, compared with 0.87 (right); 0.71 (left) in harmaline]. In the hemisphere contralateral to the master neuron, some activity was correlated to the master neurons, again showing a rostrocaudal organization with some symmetrical, spontaneous and harmaline-induced firing, as discussed in detail in the previous paper[18].

Projection method

Figure 3 projects all the cross-correlation vectors onto a two-dimensional plane for the spontaneous (spont), harmaline (harm) and picrotoxin (PTX) activity in Fig. 2. The electrode locations

corresponding to each master neuron for right (A) and left (B) hemispheres are shown. Each point is distributed unevenly on the plane but groups of points are apparent during spontaneous and harmaline-induced activity. Each point within such a group corresponds to a neuron within the same rostrocaudal band on the cerebellar cortex, as shown in Fig. 3. The right hemisphere recording area (Fig. 3A) contains a medial and a lateral rostrocaudal band, each approximately 500 μm wide. In the case of harmaline the two bands were quite distinct (Fig. 3A, harm). After picrotoxin application (Fig. 3A, PTX), the points were mixed and the grouping unclear. The distance from the origin in axis 1 indicates the mean cross-correlation. This distance was greatest after picrotoxin application due to the large mean cross-correlation (Table 1). In the left hemisphere (Fig. 3B) three groups appeared after harmaline application yet spontaneous activity showed a relatively unclear grouping on the two-dimensional plane. The width of the middle band was approximately 500 μm.

Principal component analysis

The eigenvalue calculated from the correlation matrix in principal component analysis yields the variance in spontaneous firing for a single neuron. The data in Fig. 2A for spontaneous activity is shown in Fig. 4A. Here the eigenvalues and the proportion of the total variance, eigenvalue / total summation of eigenvalue, are plotted as a function of order. By definition the eigenvalue is a monotonic decreasing function of order. The first and second components were greater than the others, but appeared to be relatively small (several %) (Table 1). This indicates that approximately 10% of the variance of spontaneous activity could be

explained according to the first and second principal components, due to their lower cross-correlation values (average 0.061 for spontaneous activity). In the case of harmaline and picrotoxin-induced activity, however, the proportion of the first and second components were comparatively large and typically accounted for more than 30 % of the variance of activity (Table 1).

Each element of the first and second eigenvectors is plotted on the same plane in Fig. 4B (data corresponding to that in Fig. 2A right, 3A spont and Fig. 4A). Elements of the first eigenvector were always positive, while elements of the second eigenvector were either positive or negative and fell into two groups. It should be noted that by definition each eigenvector was normalized to unit length.

What do eigenvalue and eigenvector in the principal component analysis suggest physiologically? The cross-correlation coefficient between any two neurons in the standard analysis can be calculated independently (eq. 1). The theory suggests that the first eigenvalue might be related to a summation of elements of the cross-correlation matrix over all possible combinations (eq. 8). Figure 4C plots the first eigenvalue as a function of the sum of cross-correlation elements (CC) excluding diagonal elements (mean cross-correlation value x number of neurons) for various experiments and animals in both hemispheres during a 96-electrode recording. The first eigenvalue correlated well with the sum of the cross-correlation elements (regression line = 0.997). Also, elements of the first eigenvector were proportionate to the mean cross-correlation value of each master neuron, as shown in Fig. 4D (regression line = 0.993). The mean cross-correlation indicates an average for neurons firing simultaneously. This

suggests that the first component reflects the degree of firing synchronicity.

The second component was related to Purkinje cell location as shown in Figs. 3 and 4B. No simple parameter describes the spatial structure of the active neurons. The mean distance of points from the center of mass of the cross-correlation vectors in N-dimensional space may reflect some characteristics of the spatial distribution of the cross-correlation perhaps being equivalent to the standard deviation of the cross-correlation. Figure 4E compares the second eigenvalue and the SD of the cross-correlation (regression line = 0.87). These results suggest that the second component represents informations related to the spatial distribution of the neurons firing in synchrony, as seen in the cross-correlation.

Spatiotemporal patterns of firing

The raster display in Fig. 5A represents spontaneous activity in Purkinje cells in the right hemisphere (cells as in Fig. 2A). Each line (row) shows the pattern of neuronal activity in a single neuron over an 2.5 sec period. A pair of four lines from upper side in the Figure arrayed four corresponding neurons of one column from rostral to caudal side in real recording location. Climbing fiber bursts lasted about 100 msec, blocking in space[11,12] occasionally, although most of the neurons did fire simultaneously at some moment.

These temporal and spatial firing patterns were relatively complex. Principal component analysis can be used, however, to induce a "typical" temporal and spatial pattern. Each principal component in the time domain is given by eq. (7). Elements of the eigenvector in the equation can be used as weighting factors for the

raw data. Figure 5B shows the first (Fig. 5Ba) and second (Fig. 5Bb) components for the data in Fig. 5A. It should be noted that the standardized data, as defined by eq. (5), was used. Since each element of the first eigenvector was positive (Fig. 4B), Figure 5Ba has the largest values whenever many neurons fire simultaneously. This suggests that the first component is related to the synchronicity of neuronal activity.

Since the elements of the second eigenvector were either positive or negative (Fig. 4B), the second component is more complex. When neurons were active in the lateral site (lower lines in Fig. 5A), the second component was large while activity in the medial neurons (upper in Fig. 5B) yielded lower or negative values. This suggests that the second component may reflect spatial pattern information. It should be noted that by definition the first and second components are not correlated with each other. Figure 5C shows a two-dimensional representation of the first and second components of possible patterns over all neurons. When points were separated from each other, the spatial firing patterns differed. The climbing fibers activated different groups of Purkinje cells at a different times. Thus each point in Fig. 5C represents both temporal and spatial information.

Effects of harmaline and picrotoxin

From the above analysis it is suggested that the first and second components reflect synchronicity and the spatial information of the firing activity, respectively. The effects of harmaline (harm) and picrotoxin (PTX) on the first, second and third eigenvalues in a pair of 64- and 96-electrode experiments are shown in Fig. 6. The proportion of the first component was

increased by both harmaline and picrotoxin (Fig. 6A). However, the contribution of the second component was increased by harmaline and decreased by picrotoxin in some cases (Fig. 6B). This may be due to the effects of harmaline to enhance the synchronous firing of rostrocaudal bands of Purkinje cells while these disappeared in the presence of picrotoxin. The third components were not significantly affected by these drugs (Fig. 6C).

DISCUSSION

Characteristics of sampling data

In our analysis, climbing fiber activity at a moment was represented in a data matrix with 96 bits (Purkinje cells), as shown in eq. (4), with a sampling interval of 1 or 10 msec. Sampling at very short intervals resulted in many zero- or one-bit sets in the momentary data. On the other hand, sampling at long intervals yielded almost no zero bit sets due to a high probability of simultaneous firing. This procedure also affected the standardization variable and the value of the cross-correlation coefficient in the principal component analysis. The cross-correlation coefficients were larger with longer sampling intervals. It should be noted that principal component analysis does not yield an exact relationship among neurons if there is a time lag in the peak of the cross-correlation histogram. Since the time lag in these experiments was within 10 msec[18], this is not a factor and analysis of data samples at 10 msec may reflect the actual spatial and temporal relationship among the analyzed neurons.

Projection method

Some simplification is clearly required in order to understand the complex temporal and spatial relationships within a population of active neurons. The projection of cross-correlation vectors to lower dimensional space indicated clear groupings in the distribution of active neurons, as shown in Fig. 3. Since the distance between any two vectors reflected a similarity in the spatial distribution of the cross-correlation coefficients, neurons within the same group could have similar spatiotemporal firing patterns. It is known that the spontaneous climbing fiber activity occurs in 500 μm rostrocaudal bands in Crus IIA of rat cerebellar cortex[16]. The projection method revealed parallel relationships among neurons as shown in Fig. 3.

Principal component analysis

Principal component analysis may be used to extract a few fundamental characteristics of spatiotemporal firing patterns. There is a difference, however, between electrophysiological activity data and data in the standard statistical textbooks. In statistical analysis, raw data does not include null sets. However, neuronal data have null points whenever all the sampled neurons are silent. For example, during spontaneous activity, more than half of the data points were null at a 10-msec sampling interval. Since null data is not meaningless and may not be omitted, the question of sampling distribution must be addressed. This is most evident when the firing frequency of all the neurons is low. The question of the time domain remains unsolved in theory probably because null data is also involved in this analysis. We can of course apply standard principal component analysis to our data, in which case the null patterns are skipped or compressed. But in this case

the correlation matrix might differ from those described above and the temporal information of the neuronal activity will certainly be lost.

Using principal component analysis, only a small percentage of variance could be interpreted during spontaneous firing, as shown in Fig. 4A and Table 1. This may be due to the low mean of the cross-correlation coefficients. In the presence of harmaline and picrotoxin, more than 30 % of the variance could be interpreted in light of the first and second components (Table 1).

The first eigenvalue can be estimated, assuming that the correlation matrix is uniform as described in the Methods. In the picrotoxin experiment, the cross-correlation matrix was close to uniform, which was equivalent to a lower ratio of (mean SD)/(mean cross-correlation). Figure 4C showed that the first eigenvalue was related to the sum of the element of cross-correlation matrix or the mean cross-correlation value. Since the mean cross-correlation indicates a degree of synchronicity in firing, the first component may be related to synchronicity in firing. This was also supported by the temporal variation of the first component, as shown in Fig. 5Ba. In statistical analysis the first component describes size.

Figure 4D demonstrated that each component of the first eigenvector was well-correlated to mean cross-correlation value of each corresponding neuron. This suggests that the first eigenvector is directed to the center of the mass of the correlation vectors in N-dimensional space.

Theory indicates that the second eigenvector is perpendicular to the first eigenvector and that the second eigenvalue gives the variance of the data projected onto the second eigenvector. This suggests that the second component is related to spreading of the

correlation vectors. One possible indicator of such spreading could be the standard deviation from the mean corresponding to the center of the mass. Figure 4E, showing the second eigenvalue, could be explained in this way. The fitness on the regression line in Fig. 4E depends on the ratio of the second eigenvalue to the third eigenvalue. If the second eigenvalue is almost identical to the third, the vectors will be distributed within the circle and the spreading is not approximated by the SD. In this case, two-dimensional projection does not represent a complete relationship and three-dimensional space might be preferable. The second component is defined by the shape factor in statistics.

Beyond the third, components do not contribute significantly to the variance because the proportion is small, as shown in Fig. 4A. Therefore the third component in Fig. 6 is not an effective representation of characteristics of the data set.

Comparison to other analyses.

There are several methods for the analysis and representation of spatiotemporal firing patterns of groups of neurons. If only a few electrodes are used in an experiment, paired cross-correlation coefficients provide a useful and precise representation of the relationships among the neurons[15,19]. This method is clearly inadequate for studying nearly 100 electrodes. We consider several other methods below.

The most direct analysis would involve analyzing the spatial pattern of activity for each point in time. Theoretically, different 2^N combinations exist in the N-different neurons recorded. We surmise that this method is too direct and the results would be difficult to analyze and interpret.

A second method of analysis involves plotting the center of the mass from an entire array of paired cross-correlations, with the coordinate of:

$$R_i = \frac{\sum_{j<i}^{N} C_{ij} r_j}{\sum_{j<i}^{N} C_{ij}}$$

where r_j is a real coordinate of the j-th master neuron on the recording area[17]. When there are clear groupings on neuronal activity, this type of plot might show some grouping on the plane. It could be speculated that when each neuron displayed a close correlation to another, the distribution of each point could concentrate on the center of the plane and mix to background points.

The third method to apply standard clustering tools[7]. We can calculate Euclidian distance between paired cross-correlation vectors in N-dimensional space. From this distance, similar groupings are represented by a tree structure. When many neurons are involved, however, this representation becomes complicated although it may yield similar results for grouping.

The fourth is to apply metric multidimensional scaling to the correlation matrix[10]. This analysis is very useful as compared with the three applications mentioned above when all the neurons are similarly correlated to each other. However, this method is sensitive to small differences among neuron groups. For example, if a neuron has a different firing pattern from the others due to electrode or recording conditions, this procedure will emphasize the difference.

In conclusions, we have applied several methods to analyze data obtained during multiple electrode recording experiments. The projection method and the so-called principal component analysis were shown to be useful tools in the analysis and representation of some effective variables involved in complex spatiotemporal firing patterns. These analyses should be developed in further studies since multiple electrode recording could become one of most useful tools for the study of neuronal organization.

REFERENCES

1. Bach M. and Krüger J. (1986) Correlated neuronal variability in monkey visual cortex revealed by a multi-microelectrode. Exp. Brain Res. 61, 451-456.

2. Barth D.S. and Di S. (1991) Laminar excitability cycles in neocortex. J. Neurophysiol. 65, 891-898.

3. Bieber, S.L. and Smith D.V. (1986) Multivariate analysis of sensory data: a comparison of methods. Chemical Senses 11, 19-47.

4. Fukuda M., Yamamoto T. and Llinás R. (1987) Simultaneous recordings from Purkinje cells of different folia in the rat cerebellum and their relation to movement. Soc. Neurosci. Abstr. 13, 603.

5. Gerstein G.L., Perkel D.H. and Dayhoff J.E. (1985) Cooperative firing activity in simultaneous recorded populations of neurons: Detection and measurement. J. Neurosci. 5, 881-889.

6. Grinvald A., Frostig R.D., Lieke E. and Hildesheim, R. (1988) Optical imaging of neuronal activity. Physiol. Rev. 68, 1285-1366.

7. Johnson R.A. and Wichern D.W. (1982) Applied Multivariate Statistical Analysis, Prentice-Hall, Englewood Cliffs, NJ.

8. Kitazawa S. (1990) Application of principal component analysis for characterizing convergence patterns of inputs in interneurons of the cat forelimb segments. Neurosci. Lett. 117, 313-318.

9. Krüger J. (1983) Simultaneous individual recordings from many cerebral neurons: Techniques and results. Rev. Physiol. Biochem. Pharmacol. 98, 117-233.

10. Kruskal J.B. (1964) Non-metric multidimensional scaling: A numerical method. Psychometrika 29, 115-129.

11. Llinás R. (1974) 18th Bowditch Lecture: Motor aspects of cerebellar control. Physiologist 17, 19-46.

12. Llinás R., Baker R. and Sotelo C. (1974) Electrotonic coupling between neurons in cat inferior olive. J. Neurophysiol. 37, 560-571.

13. Llinás R. and Sasaki K. (1989) The functional organization of the olivo-cerebellar system as examined by multiple Purkinje cell recordings. Eur. J. Neurosci. 1, 587-602.

14. Morrison D.F. (1976) Multivariate statistical methods. McGraw-Hill, NY.

15. Perkel D.H., Gerstein G.L. and Moore G.P. (1967) Neuronal spike trains and stochastic point processes. II. Simultaneous spike trains. Biophys. J. 7, 419-440.

16. Sasaki K., Bower J.M. and Llinás R. (1989) Multiple Purkinje cell recording in rodent cerebellar cortex. Eur. J. Neurosci. 1, 572-586.

17. Yamamoto T., Fukuda M. and Llinás R. (1986) Bilateral synchronization of climbing fiber activity. Soc. Neurosci. Abstr. 12, 577.

18. Yamamoto T., Fukuda M. and Llinás R. (1992) Bilateral synchronium in the rat cerebellar cortex. submitted.

19. Yamamoto M. and Nakahama H. (1983) Stochastic properties of spontaneous unit discharges in somatosensory cortex and mesencephalic reticular formation during sleep-waking stages. J. Neurophsyiol. 49, 1182-1198.

Figure legends

Fig. 1. Schematic model for analysis in multiple electrode recordings. A. Projection method to represent whole relationship within an entire set. a, schematic spatial mapping of cross-correlation coefficients to a master neuron M. Size of dots indicates degree of cross-correlation coefficient. In this model dots with higher values comprise a grouping and transversely distribute. b, elements of cross-correlation vector to the i-th neuron. N, number of neurons recorded. c, projection of cross-correlation vectors on two-dimensional plane from N-dimensional space. B. Geographical model of principal component analysis. a, raster display of raw data as a function of time. Each dot indicates firing of one neuron during one sampling interval. Each row line shows a time sequence for activity of one neuron. ch, channel (electrode). b, firing pattern at a moment as a vector in which component is shown by bit pattern, c, Upper, vector representation of a whole sampling data in N-dimensional space. Lower, projection of vectors on two-dimensional plane from N-dimensional space.

Fig. 2. Spatial distribution of cross-correlation coefficients using 96-electrode bilateral recording. Sampling interval, 10 msec. A. Representation of coefficient value of cross-correlation to one master neuron, M, in right hemisphere (right) in the spontaneous state (spont), harmaline (harm) and picrotoxin (PTX) applications. Radius of dots indicates degree of cross-correlation. Higher region in cross-correlation shows rostrocaudal band structure in spontaneous state and harmaline and some symmetrical properties to contralateral hemisphere (left). Distribution in case of the PTX is

relatively uniform. Upper site, rostral. Spacing among each neuron, 166 μm. B. Recording site. Climbing fiber activities of 96 electrodes were recorded from bilateral Crus IIA of rat cerebellar cortex. Tentative recording ratio to Purkinje cells was 16% using #150 electromicroscopic grid

Fig. 3. Projection of cross-correlation vector to two-dimensional plane in right (A) and left (B) hemispheres in cases of spontaneous state (spont), harmaline (harm) and picrotoxin (PTX) applications. Data were the same as Fig. 2. Each dot connects to real recording location. Distribution of each dot shows a whole relationship within an entire neuron set. In the spontaneous state (spont in A), two groups appear in right hemisphere (surrounded by rings). In harmaline (harm in A), separation between groups becomes more clear, but in picrotoxin (PTX in A), mixed. In the left hemisphere (B), there are three groups in case of harmaline (harm in B). Mesh in lower site, real electrode location (48 electrodes) in both hemispheres. Ordinate, first axis; abscissa, second axis.

Fig. 4. Relationships among eigenvalue, eigenvector and cross-correlation. A. Eigenvalue and cumulated percentages of proportion of total variance. First eigenvalue is the largest and the subsequent values are in decreasing order. Ordinate, eigenvalue (left); cumulated % (right). Abscissa, order. B. Simultaneous representation of elements of the first and second eigenvectors on the same plane. All elements of the first eigenvector are positive. Elements of the second eigenvector are either positive or negative. Abscissa, element of the first eigenvector. Ordinate, element of the

second eigenvector. C. First eigenvalue as a function of summation of cross-correlation over all possible combinations in different experiments. Cross-correlation coefficient of regression line, r = 0.997. CC, cross-correlation. Ordinate, first eigenvalue. Abscissa, summation of cross-correlation. D. Elements of the first eigenvector to mean cross-correlation value of the corresponding neurons. Cross-correlation coefficient of the regression line, r = 0.993. Ordinate, elements of the first eigenvector. Abscissa, mean cross-correlation value to the corresponding master neuron. E. Second eigenvalue as a function of standard deviation (SD) of cross-correlation over all possible combinations, that is, corresponding to the mean spreading of the distribution from the center of the mass on cross-correlation vector. Correlation coefficient of regression line, r = 0.83. Ordinate, second eigenvalue; abscissa, SD of the cross-correlation.

Fig. 5. Spatiotemporal relations of spontaneous firing in right hemisphere. Sampling interval, 10 msec. A. Raster display of the real spontaneous firing during 2.5 sec. Each line (row) shows a raw temporal patterns of firing of one neuron as a function of time. Upper site, medial; lower site, lateral in right hemisphere. B. First (a) and second (b) principal components as a function of time to the above corresponding data. a, first component. Peak value in histogram is approximately proportional to number of active neurons. b, second principal component. The values are large when neurons are active in the lateral site. C. Simultaneous representation of the first and second principal components. Spatiotemporal characteristics of firing at a moment are approximated to one point in the principal component analysis.

Fig. 6. Effect of variance (%) of the first (A), second (B) and third (C) components to spontaneous state (spont), harmaline (harm) and picrotoxin (PTX). The first components increased to harmaline and picrotoxin applications. The second component decreased by picrotoxin in some cases. The third component did not change so much. Open, right hemisphere; filled, left hemisphere. Triangle, 64 electrodes; circle, 96 electrodes. Ordinate, proportion (%) of the eigenvalue. Abscissa, drugs.

Fig. A. Distribution of elements of the first, second and third eigenvectors under various conditions corresponding to Table A.

Table 1. Mean values of spontaneous frequency, cross-correlation coefficient and principal component for 64- and 96-electrode recordings.

CH	Site	Drug	N	Freq	CC	SD	Eigenvalue					
							First	(%)	Second	(%)	Third	(%)
64	r	spont	7	2.6	0.033	0.037	2.0	(7.6)	1.4	(5.4)	1.2	(4.5)
	r	harm	9	3.5	0.076	0.052	3.2	(11.4)	1.6	(5.7)	1.3	(4.7)
	r	PTX	6	5.9	0.195	0.095	6.5	(22.5)	2.1	(7.3)	1.6	(5.6)
	l	spont	7	2.6	0.040	0.043	2.4	(8.2)	1.5	(5.3)	1.2	(4.3)
	l	harm	9	3.1	0.070	0.069	3.1	(11.6)	1.7	(6.5)	1.4	(5.5)
	l	PTX	4	5.3	0.195	0.100	6.0	(22.5)	2.1	(8.2)	1.5	(5.9)
96	r	spont	8	2.5	0.053	0.048	3.1	(8.9)	1.7	(4.8)	1.3	(3.8)
	r	harm	8	4.2	0.148	0.101	6.8	(18.6)	2.6	(6.9)	1.8	(4.8)
	r	PTX	4	4.2	0.218	0.108	9.5	(25.5)	2.3	(6.2)	1.6	(4.3)
	l	spont	8	2.0	0.043	0.048	3.1	(7.5)	1.9	(4.5)	1.5	(3.7)
	l	harm	8	4.0	0.150	0.098	7.5	(18.3)	2.9	(7.0)	2.0	(5.0)
	l	PTX	4	4.4	0.203	0.100	9.2	(22.9)	3.4	(8.3)	2.1	(5.1)

Abbreviation: CH, number of cells recorded; r, right site; l, left site; spont, spontaneous state; harm, harmaline; PTX, picrotoxin; N, numper of sample; Freq, mean spontaneous frequency over all cells; CC, mean cross-correlation coefficients; SD, mean standard deviation of the cross-correlation

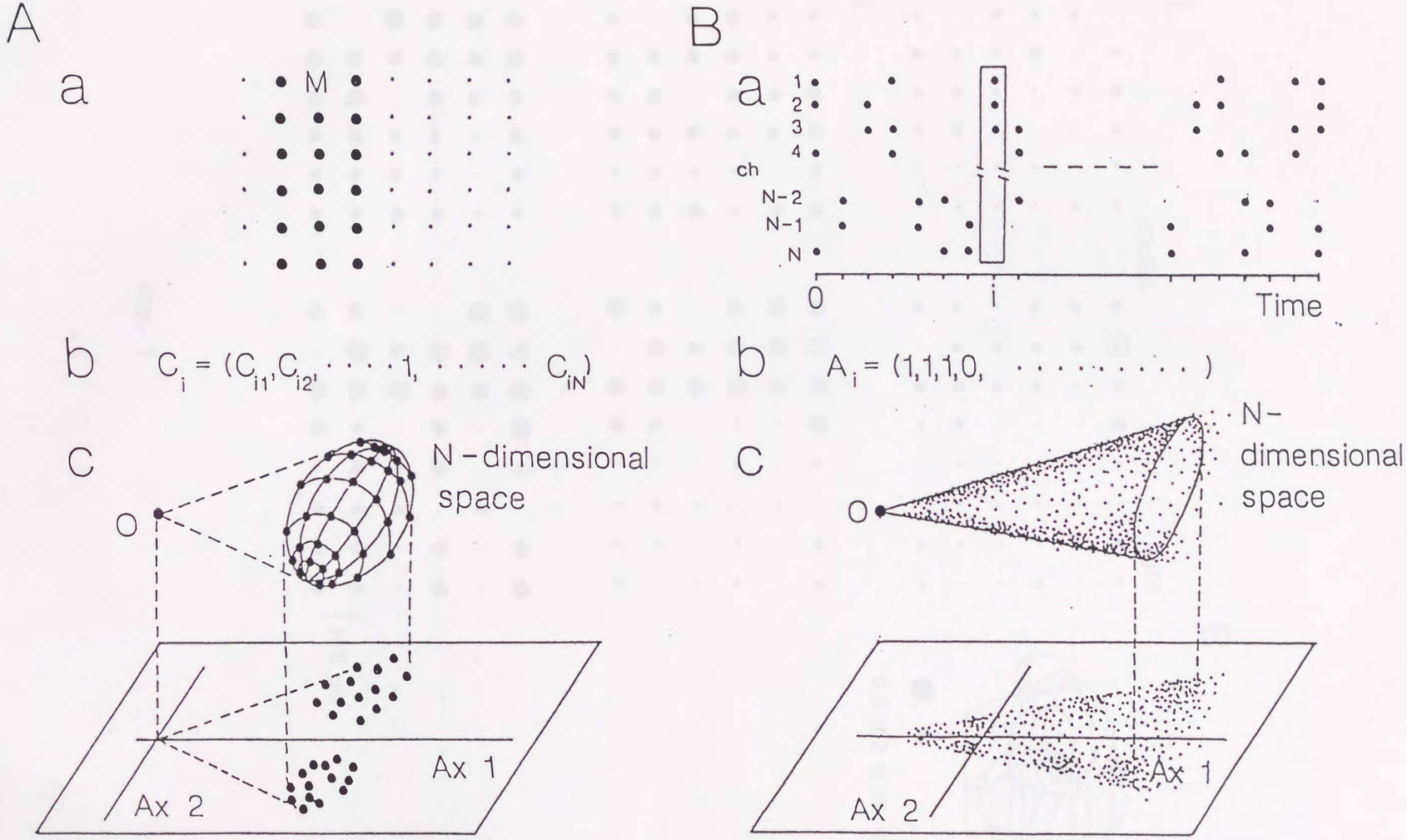
A
a
M
b
$C_i = (C_{i1}, C_{i2}, \cdots 1, \cdots\cdots C_{iN})$
c
O
N-dimensional space
Ax 1
Ax 2
B
a
1
2
3
4
ch
N-2
N-1
N
0
i
Time
b
$A_i = (1,1,1,0, \cdots\cdots\cdots)$
c
O
N-dimensional space
Ax 1
Ax 2

Fig. 1

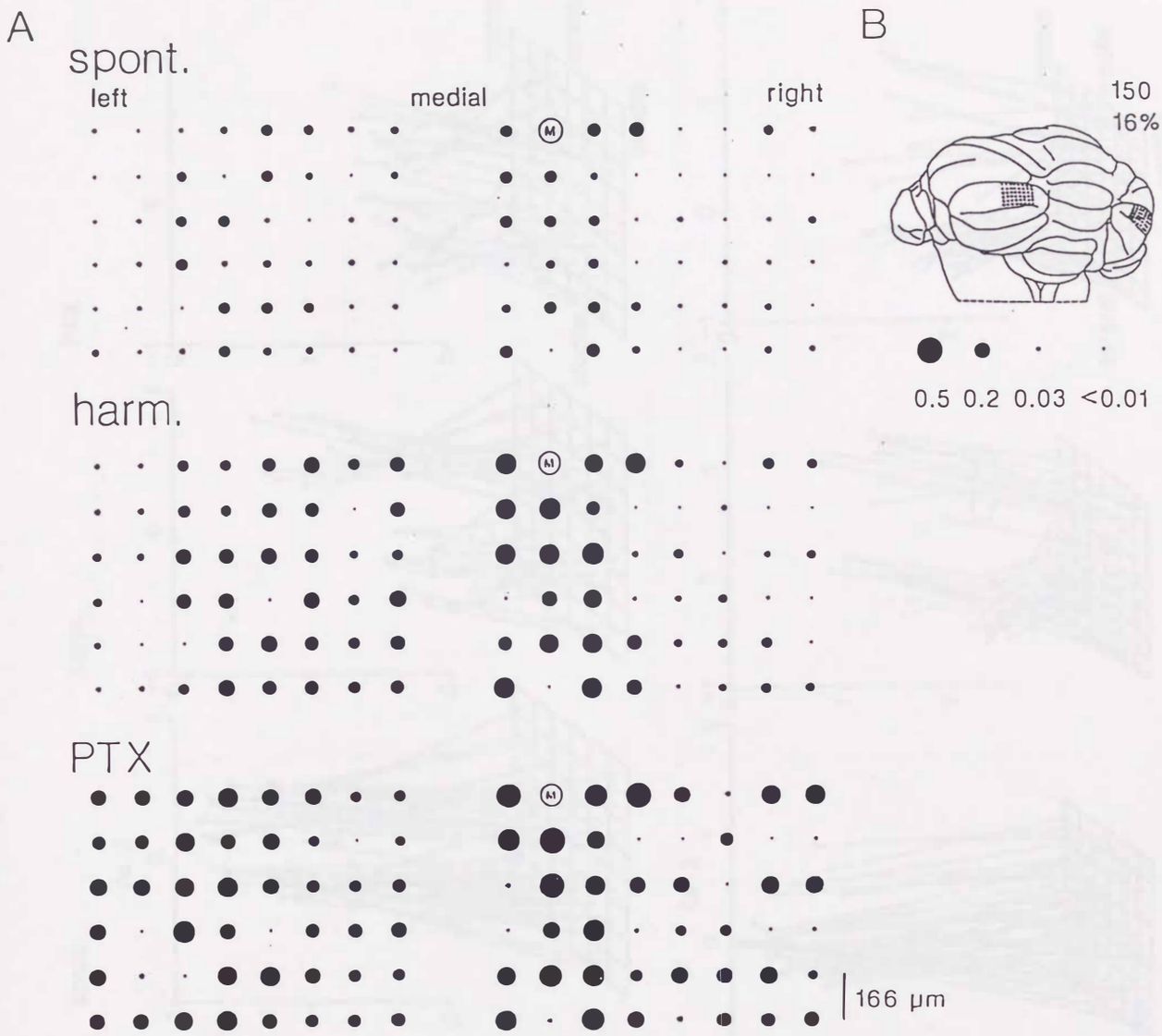

Fig. 2

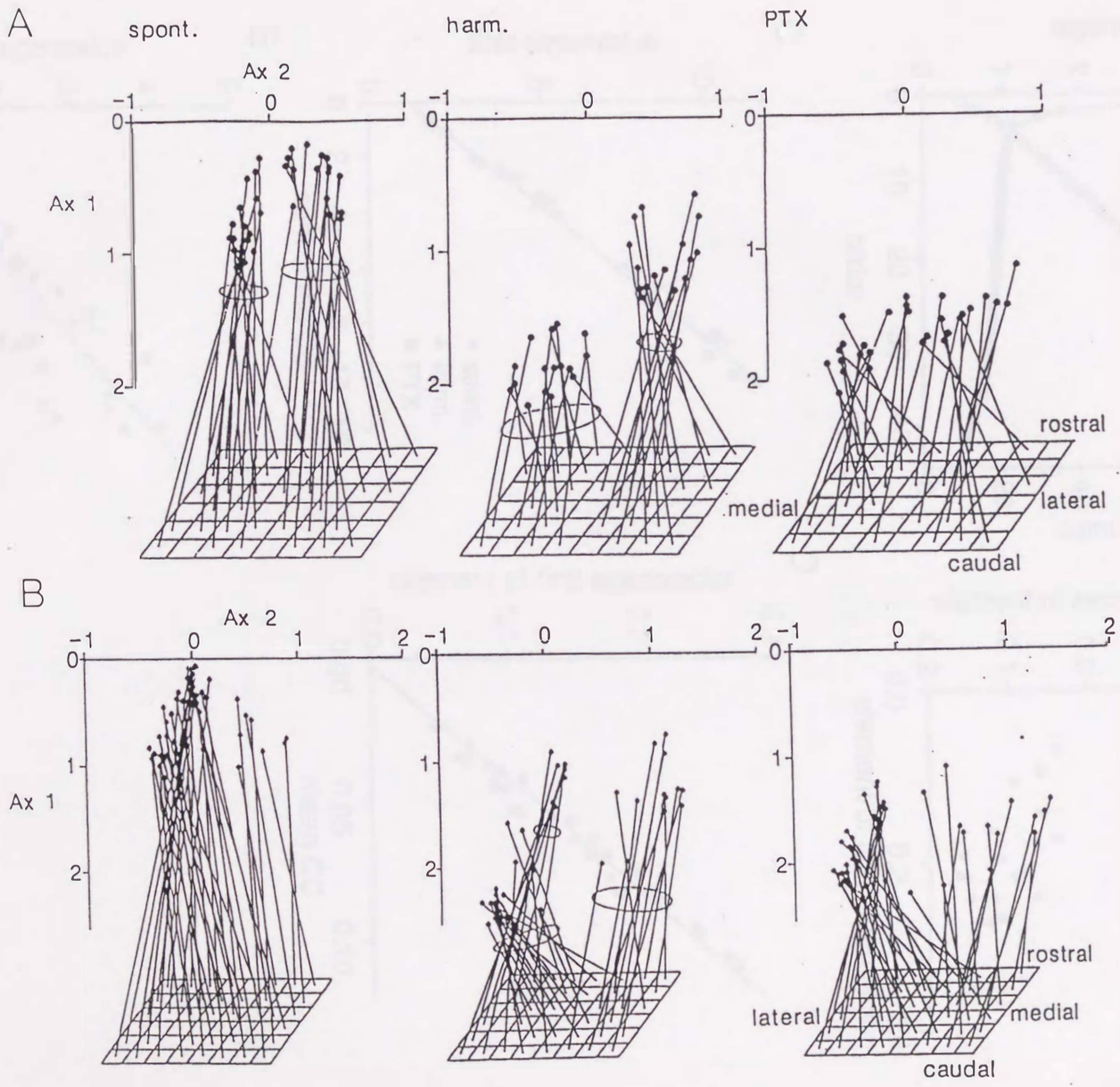
A
spont.
harm.
PTX
Ax 2
Ax 1
rostral
medial
lateral
caudal
B
Ax 2
Ax 1
rostral
lateral
medial
caudal

Fig. 3

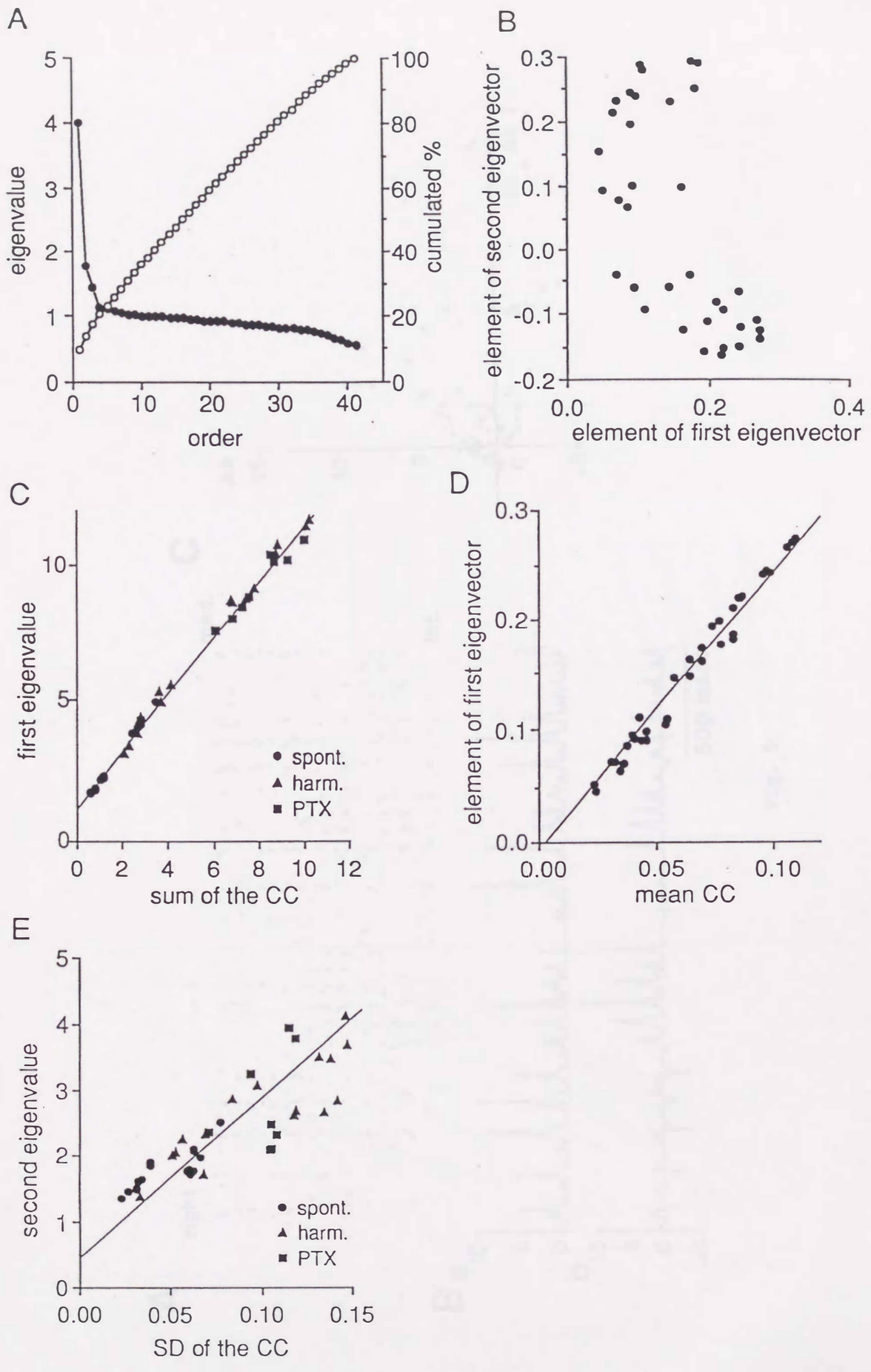
A
eigenvalue
cumulated %
order
B
element of second eigenvector
element of first eigenvector
C
first eigenvalue
sum of the CC
spont.
harm.
PTX
D
element of first eigenvector
mean CC
E
second eigenvalue
SD of the CC
spont.
harm.
PTX

Fig. 4

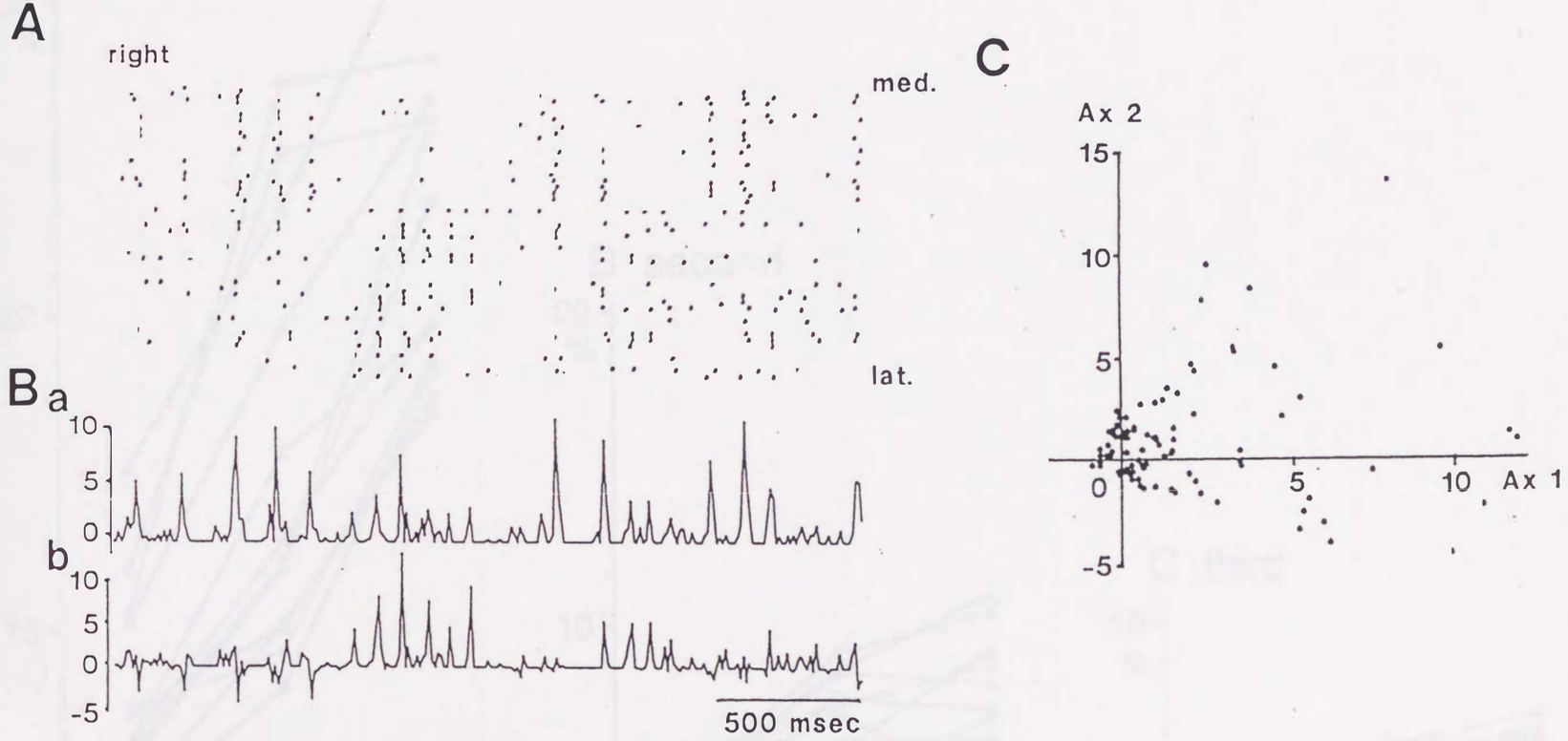

Fig. 5

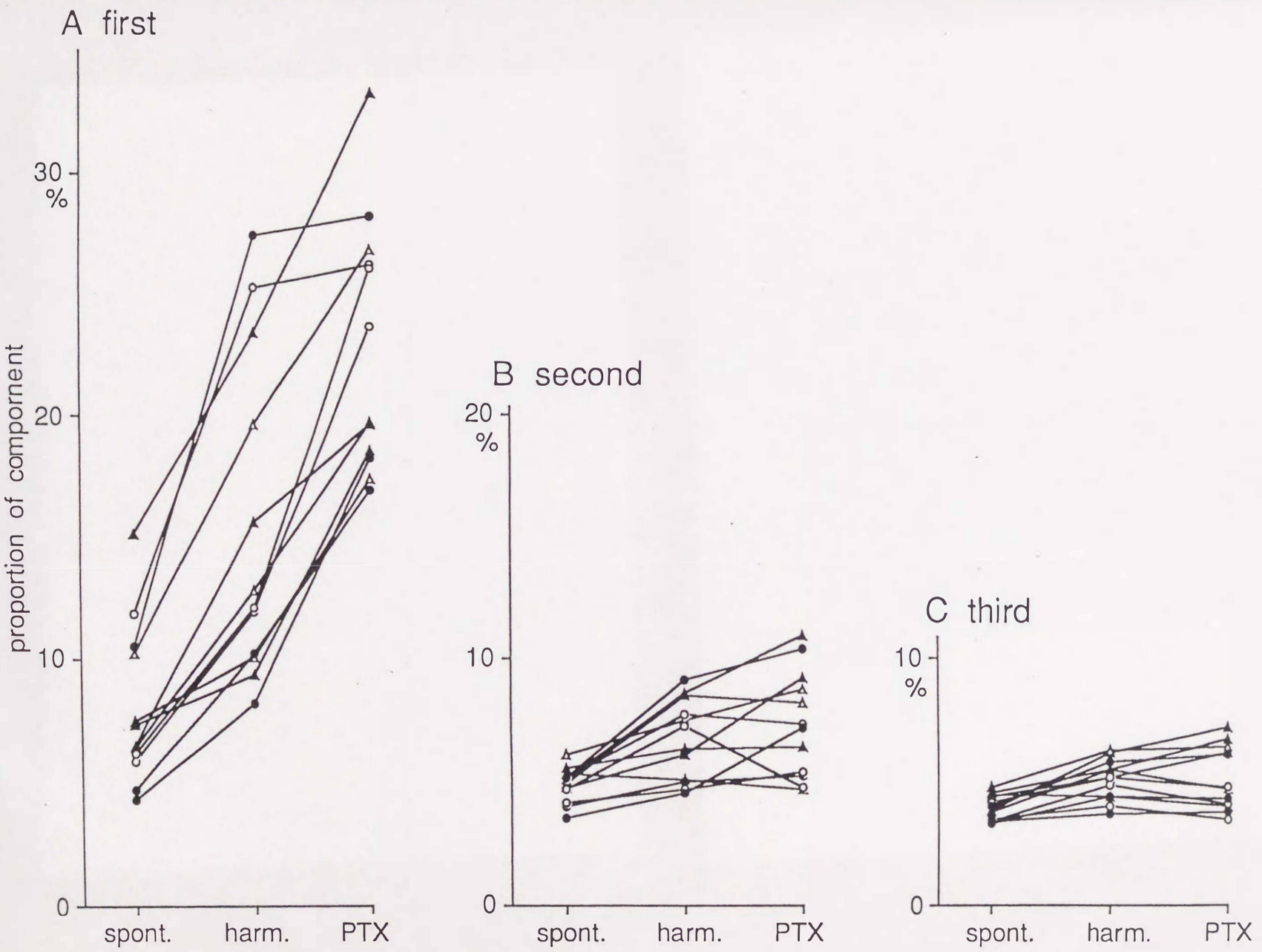
A first
B second
C third
proportion of component
30 %
20
10
0
20 %
10 %
spont.
harm.
PTX

Fig. 6

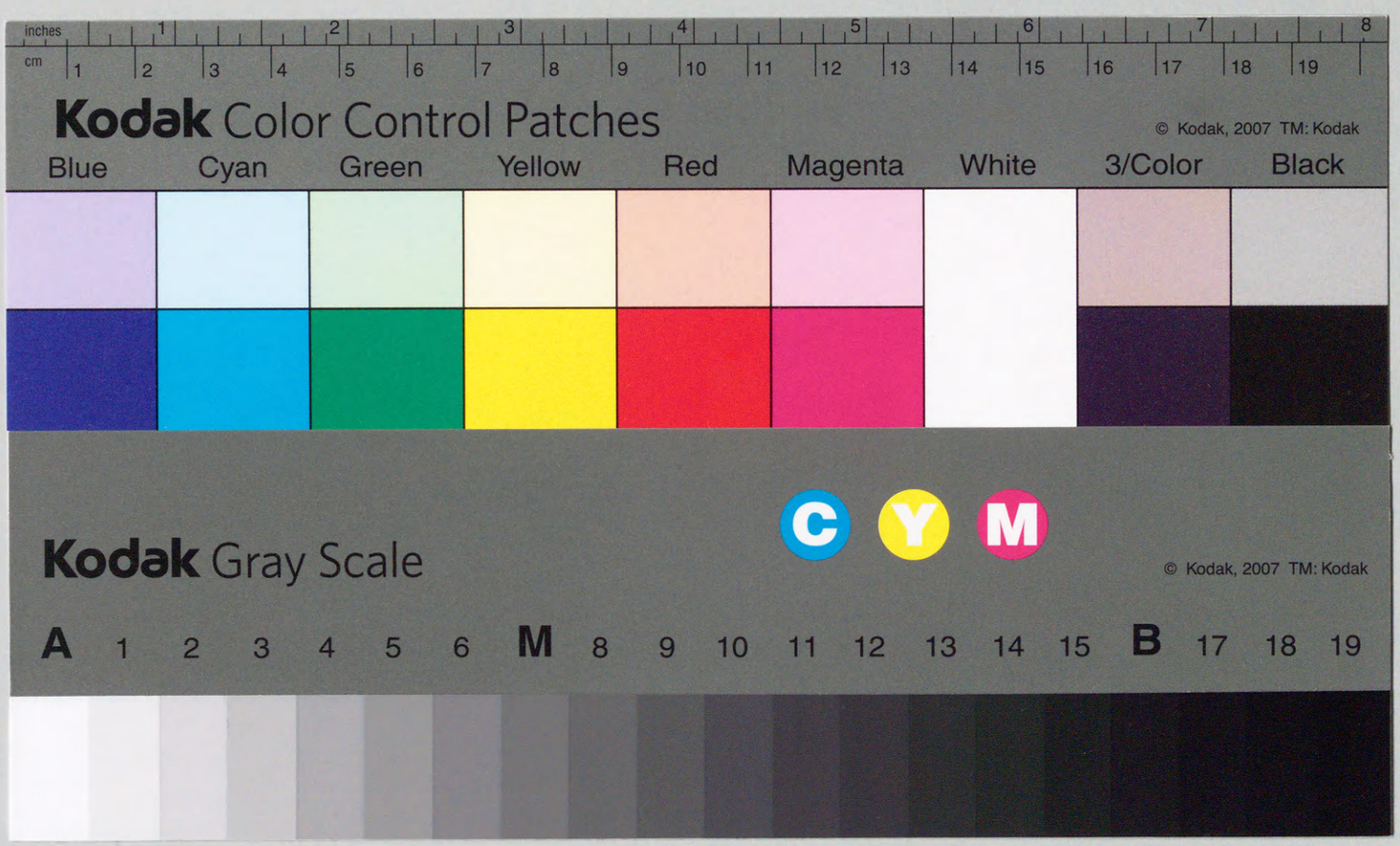
inches
cm
Kodak Color Control Patches
© Kodak, 2007 TM: Kodak
Blue
Cyan
Green
Yellow
Red
Magenta
White
3/Color
Black
Kodak Gray Scale
C
Y
M
© Kodak, 2007 TM: Kodak
A 1 2 3 4 5 6 M 8 9 10 11 12 13 14 15 B 17 18 19